© 2024 Hefei Institutes of Physical Science, Chinese Academy of Sciences and IOP Publishing Printed in China
Plasma Science and Technology

Plasma Sci. Technol. **26** (2024) 075402 (9pp) https://doi.org/10.1088/2058-6272/ad31ef

Effect of coil and chamber structure on plasma radial uniformity in radio frequency inductively coupled plasma

Yang ZHAO (赵洋)[1], Xiaohua ZHOU (周晓华)[1,*], Shengrong GAO (高升荣)[1], Shasha SONG (宋莎莎)[1] and Yuzhen ZHAO (赵玉真)[2]

[1] Shaanxi International Joint Research Center for Applied Technology of Controllable Neutron Source, Xijing University, Xi'an 710123, People's Republic of China
[2] Technological Institute of Materials & Energy Science (TIMES), Xi'an Key Laboratory of Advanced Photo-electronics Materials and Energy Conversion Device, School of Electronic Information, Xijing University, Xi'an 710123, People's Republic of China

[*]E-mail of corresponding author: zhouxiaohua@xijing.edu.cn

Received 13 January 2024, revised 7 March 2024
Accepted for publication 8 March 2024
Published 16 May 2024

Abstract

Enhancing plasma uniformity can be achieved by modifying coil and chamber structures in radio frequency inductively coupled plasma (ICP) to meet the demand for large-area and uniformly distributed plasma in industrial manufacturing. This study utilized a two-dimensional self-consistent fluid model to investigate how different coil configurations and chamber aspect ratios affect the radial uniformity of plasma in radio frequency ICP. The findings indicate that optimizing the radial spacing of the coil enhances plasma uniformity but with a reduction in electron density. Furthermore, optimizing the coil within the ICP reactor, using the interior point method in the Interior Point Optimizer significantly enhances plasma uniformity, elevating it from 56% to 96% within the range of the model sizes. Additionally, when the chamber aspect ratio k changes from 2.8 to 4.7, the plasma distribution changes from a center-high to a saddle-shaped distribution. Moreover, the plasma uniformity becomes worse. Finally, adjusting process parameters, such as increasing source power and gas pressure, can enhance plasma uniformity. These findings contribute to optimizing the etching process by improving plasma radial uniformity.

Keywords: inductively coupled plasma, fluid simulation, optimized coil, chamber aspect ratio, plasma uniformity

(Some figures may appear in colour only in the online journal)

1. Introduction

Inductively coupled plasma (ICP) sources have extensive applications across diverse industries due to their unique advantages, which include a simple device structure and the ability to generate higher plasma density and ion flux at low temperature and gas pressure conditions. For instance, ICP has found applications in plasma etching and thin film deposition in semiconductor manufacturing [1–4], ion thrusters in aerospace [5, 6], and neutral beam injection technology within the domain of nuclear fusion [7–9]. With the advancement of high technology, the demand for ICP sources has escalated across all sectors. Particularly within the integrated circuit industry, there is a pressing need to meet market demands for larger wafer sizes, driving the urgency for ICP sources capable of generating expansive and uniform plasma to mitigate production costs and improve production efficiency.

In recent years, many experimental and theoretical studies have found that plasma uniformity can be modulated by adjusting coil parameters and chamber structure in ICP sources [10–14]. Sun *et al* performed fluid simulations to

[*] Author to whom any correspondence should be addressed.

investigate the effects of coil placement and dielectric window shape on plasma density distribution [10]. Their results indicate that modifying the gradient coil configuration and precisely controlling the power and pressure within an ICP system can significantly improve plasma uniformity. For large-area ICP, Son *et al* used self-consistent simulations to optimize plasma uniformity [11]. Their research showed that reducing the chamber aspect ratio is beneficial for optimizing plasma uniformity. However, excessively low aspect ratios also induce an M-shaped distribution in electron density, consequently leading to inadequate plasma uniformity. Xiao *et al* achieved control over plasma uniformity by independently regulating the input power of the inner and outer spiral coils, thereby enhancing plasma etching uniformity [12]. Lu *et al* found that the plasma radial uniformity is improved as the outer coil current changes from 5.7 to 7.7 A, inducing a transition in ion density from a center-high to an edge-high distribution in the two-dimensional fluid simulation. Moreover, the best plasma uniformity was achieved when the coil current was set at 6.7 A [13]. Collison *et al* conducted a hybrid model study. They found that plasma uniformity is improved by reducing the number of the coil turns, such as a three-turn coil, but at the expense of reduced electron density [14].

In addition, modulation of plasma uniformity can also be achieved by changing process parameters, such as source power and dual frequency [15–19], as demonstrated in the following referenced studies. Using a combination of simulations and experiments, Kim *et al* discovered that using dual frequencies with a radio frequency power ratio of 1 (2 MHz) to 5 (13.56 MHz) yielded superior plasma uniformity compared to using a single frequency [15]. Gweon *et al* used the dual comb-type ICP source to assess plasma uniformity under dual frequencies. The results indicated improved plasma uniformity with increased single-frequency source power at 5 kW and 13.56 MHz. Furthermore, plasma uniformity was enhanced further by incorporating a 2 MHz source power of 0.9 kW to form a dual-frequency mode [16]. Yang *et al* studied the influence of dual frequency in ICP Ar/CF_4 discharge on plasma uniformity. The findings suggested superior plasma uniformity was achieved with dual frequencies of 2 MHz and 13.56 MHz in the ICP. This improvement was attributed to an increase in electron density near the wafer edge region [18]. In addition, Levko *et al* studied the CF_4 plasma discharge, revealing that stochastic heating causes electron motions to converge near the quartz window. Consequently, the stochastic heating effect is crucial in plasma density distribution. Simulations that account for the stochastic heating of electrons yield results closer to actual experiments [19].

However, as mentioned earlier on ICP sources much of the research has focused on investigating the modulation of plasma uniformity through various process parameters, including coil parameters, chamber aspect ratio, source power and input frequency. To date, there has been no research on the effect of different coil radial spacings on plasma parameter characteristics and uniformity in ICP sources, such as step coil, isometric coil, optimized coil configurations, and discharge chamber aspect ratios. That is why systematic research and further exploration of the underlying influence mechanisms are highly desired. In addition, different coil configurations and chamber aspect ratios are effective methods [20, 21] to modulate the radial uniformity of the plasma, which have been applied in plasma etching processes [14, 22, 23]. Therefore, the two-dimensional self-consistent fluid module coupled with the electromagnetic module was selected in this study. In addition, the Interior Point Optimizer [24] in the optimization module was also utilized in the study. After utilizing the interior point approach to address optimization challenges associated with coil placement, the modulation of radial uniformity in argon discharge plasma of the ICP source was investigated by varying the coil radial distance and the discharge chamber structure. Furthermore, building upon this groundwork, the influence of discharge parameters on the ion flux and the plasma uniformity, such as source power and gas pressure, was also investigated. The results of this investigation provide reference into the design of ICP sources capable of producing large areas and uniformly distributed plasma. It is essential for the optimization of plasma etching processes.

The subsequent sections of this work are structured as follows. Section 2 gives the theoretical model including the geometric model. Moreover, the governing equations are also presented in section 2. Section 3 elucidates the results and discussion of the study, encompassing the influence of plasma radial uniformity at varying coil radial spacing, discharge chamber structure, source power, and gas pressure in radio frequency inductively coupled plasmas. Finally, the conclusions of the study are given in section 4.

2. Simulation model

2.1. Geometric model

Figure 1 illustrates the two-dimensional axisymmetric model used for simulating the ICP reactor. The reactor has five main components: vacuum, coil, dielectric window, plasma, and substrate. Plasma generation occurs within the discharge chamber, which has a radial length of 28 cm and a height of 13 cm. The radial placements of the four-turn coil are at 4 cm, 7 cm, 10 cm, and 13 cm, with a dielectric window with a height of 1 cm is placed below it.

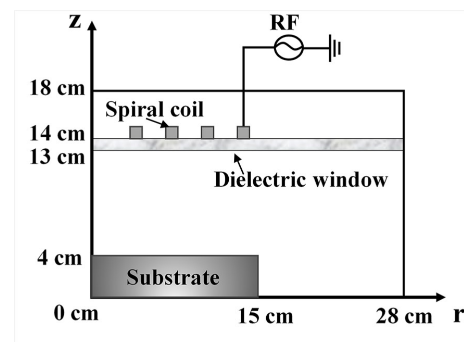

Figure 1. A two-dimensional axisymmetric model of the ICP reactor.

2.2. Governing equations

In this model, the plasma module is characterized by the continuity, momentum balance, and energy balance equations [25]. These equations coupled with the Poisson equation to calculate the density of various particles, electron temperature, flux, and the spatial distribution of the electrostatic field. We assume that the ion temperature equals the background gas temperature, eliminating the necessity to solve energy equations for ions and neutral particles [26].

The solution equations are as follows [27, 28]:

$$\frac{\partial n_e}{\partial t}+\nabla\cdot\boldsymbol{\Gamma}_e=R_e, \tag{1}$$

$$\frac{\partial n_\varepsilon}{\partial t}+\nabla\cdot\boldsymbol{\Gamma}_\varepsilon+\boldsymbol{E}\cdot\boldsymbol{\Gamma}_e=S_{en}-(\boldsymbol{u}\cdot\nabla)n_\varepsilon+\frac{Q+Q_{gen}}{q}, \tag{2}$$

where n_e represents the electron density, $\boldsymbol{\Gamma}_e$ represents the electron flux, and R_e is the electron source term of the continuity equation. Moreover, n_ε is the electron energy density, $\boldsymbol{E}$ is the electrostatic field, and $\boldsymbol{\Gamma}_\varepsilon$ represents the electron energy flux, Similarly, $\boldsymbol{u}$ is the velocity vector, which can generally be ignored. S_{en} is the electron source term of the energy balance equation, Q denotes the external heat source, and Q_{gen} refers to the generalized heat source.

Since no bias source is applied, it is assumed that the plasma satisfies the electrical neutrality condition, that is, the electron density n_e equals the ion density n_i.

$$n_e=n_i. \tag{3}$$

Because of the small mass of the electron, the drift-diffusion equation is used to solve for the electron flux $\boldsymbol{\Gamma}_e$ and the electron energy flux $\boldsymbol{\Gamma}_\varepsilon$.

$$\boldsymbol{\Gamma}_e=-(\mu_e\cdot\boldsymbol{E})n_e-D_e\cdot\nabla n_e, \tag{4}$$

$$\boldsymbol{\Gamma}_\varepsilon=-(\mu_\varepsilon\cdot\boldsymbol{E})n_\varepsilon-D_\varepsilon\cdot\nabla n_\varepsilon, \tag{5}$$

here, μ_e and D_e represent the electron mobility and diffusivity, respectively. μ_ε and D_ε denote electron energy mobility and diffusivity, respectively.

The following Poisson equation is employed to solve the electrostatic field:

$$\nabla^2\varphi=-\frac{e}{\varepsilon_0}(n_i-n_e), \tag{6}$$

$$\boldsymbol{E}=-\nabla\varphi, \tag{7}$$

where φ is the electric potential, and ε_0 is the dielectric constant.

The electron temperature is denoted as T_e, which can be calculated by solving the electron balance equation:

$$\frac{\partial}{\partial t}\left(\frac{3}{2}n_e k_B T_e\right)=-\nabla\cdot\boldsymbol{Q}_e-e\boldsymbol{\Gamma}_e\cdot\boldsymbol{E}+P_{ind}-W_e, \tag{8}$$

where k_B represents the Boltzmann constant, $\boldsymbol{Q}_e$ represents the electron heat flux, P_{ind} refers to the power deposition, and W_e refers to the electron loss term.

The ion density satisfies the following continuity equation:

$$\frac{\partial n_i}{\partial t}+\nabla\cdot(n_i\boldsymbol{u}_i)=S_i, \tag{9}$$

where n_i is the ion density, $\boldsymbol{u}_i$ is the velocity vector, and S_i is the source term.

Since the inductively coupled plasma source operates under low-pressure conditions, the inertial effect of the ions cannot be ignored. Therefore, the momentum balance equation of the ions is presented as follows:

$$\frac{\partial(n_i m_i\boldsymbol{u}_i)}{\partial t}+\nabla\cdot(n_i m_i\boldsymbol{u}_i\boldsymbol{u}_i)=en_i\boldsymbol{E}-k_B T_i\nabla n_i+M_i, \tag{10}$$

where m_i denotes the ion mass, T_i represents the ion temperature, and M_i represents the energy transfer resulting from the collision between ions and the background gas.

The electromagnetic field module employs the frequency domain finite difference approach to solve problems related to the induced electromagnetic field, generated by the current flowing through a coil. This approach significantly enhances the efficiency of simulations, ensuring the satisfaction of Maxwell's equations as follows [25]:

$$\nabla\times\boldsymbol{E}=-\frac{\partial\boldsymbol{B}}{\partial t}, \tag{11}$$

$$\nabla\times\boldsymbol{B}=\mu_0\boldsymbol{J}+\varepsilon_0\varepsilon_r\mu_0\frac{\partial\boldsymbol{E}}{\partial t}, \tag{12}$$

where μ_0 denotes the vacuum permeability, $\boldsymbol{J}$ denotes the current density, ε_0 refers to the vacuum dielectric constant, and ε_r refers to the relative dielectric constant.

The above equation must be applied within appropriate boundary conditions to characterize the discharge process accurately. In this work, the effect of the secondary electron emission coefficient is disregarded. Therefore, the electron flux boundary condition is obtained as follows:

$$\boldsymbol{n}\cdot\boldsymbol{\Gamma}_e=\left(\frac{1}{2}\nu_{e,th}n_e\right). \tag{13}$$

Moreover, the electron energy flux is given as follows:

$$\boldsymbol{n}\cdot\boldsymbol{\Gamma}_\varepsilon=\left(\frac{5}{6}\nu_{e,th}n_e\right). \tag{14}$$

In addition, the ion density and velocity at the boundary are zero, and the reactor walls are grounded.

3. Results and discussion

This section explores the impact of coil and chamber structures on plasma radial uniformity, primarily in the argon discharge of radio frequency ICPs. At the same time, certain studies indicate that adjusting the frequency also influences

the electron density distribution [29]. The subsequent simulation work concentrates on modulating plasma radial uniformity by adjusting coil radial spacing and chamber structures at a fixed frequency of 13.56 MHz.

First, the electron density distribution under the initial conditions of 500 W and 0.02 Torr is shown in figure 2. It can be observed that the peak electron density is 2.38 × 10^{17} m^{-3} at the chamber center. The electron density shows a center-high and edge-low distribution due to the power deposition concentrated in the chamber center under an induced electric field, resulting in poor plasma uniformity. The position of the discharge chamber center was selected from r = 0 cm to r = 15 cm as the baseline, to enhance the accuracy of evaluating plasma radial uniformity. The uniformity degree α along the radial direction is defined as follows [30, 31].

$$\alpha = \left(1 - \frac{n_{\max} - n_{\min}}{2n_{\text{ave}}}\right) \times 100\%, \quad (15)$$

where $n_{\max}$, $n_{\min}$, and n_{ave} are the peak, minimum, and mean values of the plasma density on the baseline, respectively. A larger uniformity degree α leads to better radial uniformity of the plasma. The plasma uniformity degree $\alpha \approx 56\%$ in figure 2. A large-area and uniform plasma is necessary for the plasma etching process, and deviation from this uniformity degree is undesirable. Therefore, optimizing the coil radial spacing and chamber aspect ratio is essential to improve plasma uniformity.

3.1. Effect of coil radial spacing on plasma uniformity

Adjusting the coil position induces variations in plasma density distribution. In this subsection, the number of the coil turns and axial coil position are taken as constant. Initially, the effect of different radial spacings of the coils on plasma uniformity is explored by observing the spatial distributions of various plasma parameters. Different classifications are introduced based on variations in coil radial spacing: a “step coil” if the radial spacing increases gradually, an “isometric coil” if the radial spacing remains constant, and an “optimized coil” if it is optimized using the interior point method.

Figures 3 and 4 illustrate the electron density distributions at different coil radial spacings under initial conditions of 500 W and 0.02 Torr. The graphics reveal a significant discrepancy in plasma uniformity. Specifically, the initial coil exhibits the highest electron density and the poorest uniformity among different coil configurations, as depicted in figure 3. The corresponding uniformity degree is 56%. The electron density peak is observed near the chamber center in the step coil configuration. The electron density distribution is relatively uniform in the region between r = 0 cm and r = 10 cm, gradually declining beyond that, as illustrated in figure 4(a). In this case, the plasma uniformity degree is 90%, representing an improvement of about 34% compared to the initial coil. Concurrently, the peak electron density is substantially reduced. Figure 4(b) shows similar results with isometric coil configurations. The plasma uniformity is optimal for the ICP reactor with the optimized coil configuration, as depicted in figure 4(c). The corresponding uniformity degree is 96%. However, the enhancement in uniformity comes at the expense of a decrease in

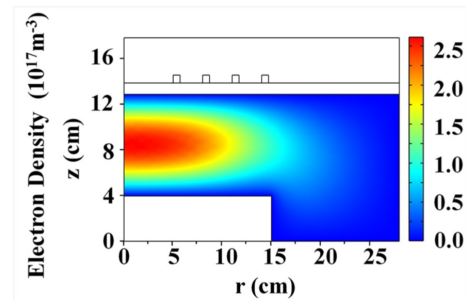

Figure 2. The electron density distribution in the initial conditions at 500 W and 0.02 Torr.

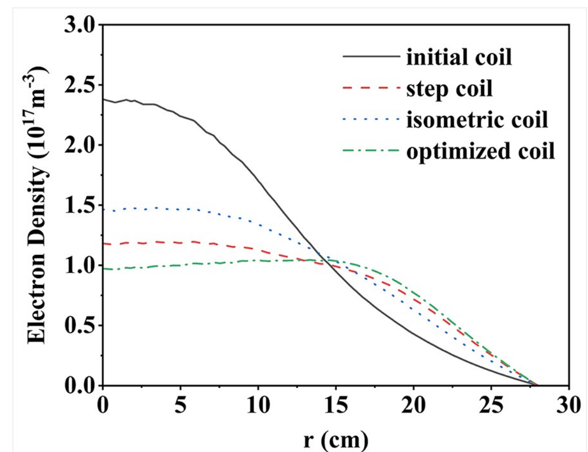

Figure 3. Radial distributions of electron density at different coil radial spacings.

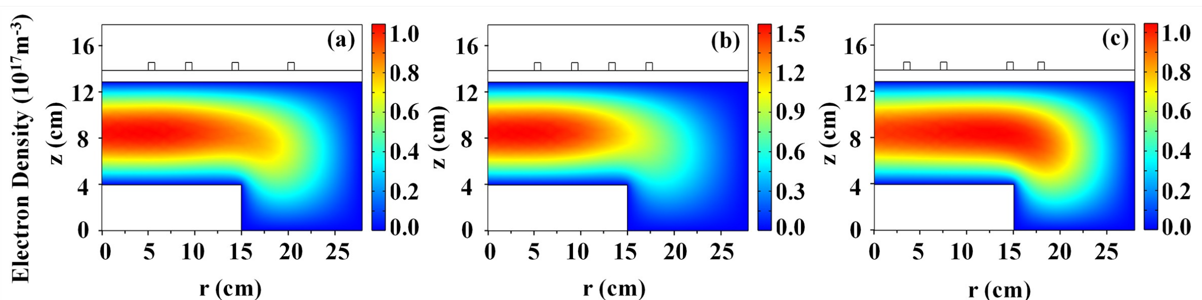

Figure 4. Distributions of electron density for different coil radial spacings. (a) Step coil, (b) isometric coil, and (c) optimized coil.

electron density.

To further investigate the impact of different coil configurations on plasma uniformity, the two-dimensional distributions of the ionization rate are depicted in figure 5. The optimized coil exhibits a uniform ionization rate distribution, while the others perform poorly. For instance, the peak ionization rate shifts outward in the step coil configuration. It reaches its maximum at r = 8 cm, where electrons are primarily active in the chamber center, and power deposition is mainly concentrated below the internal coil near the dielectric window. This phenomenon is attributed to the gradual increase in radial spacing of the step coil, leading to a corresponding attenuation of the induced electric field, as illustrated in figure 5(a).

In the case of the isometric coil, the electric field exhibits a uniform distribution, and the power deposition occurs in the region beneath the coils. Correspondingly, the ionization rate distribution tends to be concentrated toward the center region beneath the coil in figure 5(b). The ionization rate demonstrates a relatively uniform profile in figure 5(c). This uniform distribution is attained through the optimization of the coil using the interior point method. Precisely, the two outer coils are positioned away from the chamber center to modulate the reduction in plasma density at the edges. In comparison, the two inner coils are adjusted to move closer to the center. In this case, the ionization rate peak is seen below the dielectric window, where the inner and outer coils are located. Therefore, the electron density is more evenly distributed, as figure 4(c) depicts.

The ion flux is also a critical factor influencing the plasma density distribution. The ICP reactor with an optimized coil configuration is chosen as the focus of study in the following work. The source power dependence of ion flux above the substrate is plotted in figure 6(a) to investigate the effect of process parameters on the ion flux and the plasma uniformity. In this case, ranging from 200 W to 1000 W in source power, gas pressures are 0.01 Torr, 0.02 Torr, and 0.05 Torr, respectively. The ion flux shows an upward trend as source power increases. It is essential to mention that higher gas pressures lead to a faster increase of ion flux when the gas pressure is variable. The reason for this is that the plasma experiences a higher rate of electron collisions when the source power and gas pressure are raised, which in turn speeds up the process of electron ionization. Figure 6(a) also shows that increasing the ion flux from initially 0.48 × 10^{20} m^{-2} s^{-1} (at 200 W and 0.01 Torr) to 5.63 × 10^{20} m^{-2} s^{-1} (at 1000 W and 0.05 Torr). The ion flux increases as the source power increases. Consequently, the ion density increases and more ions participate in the plasma reaction. Consequently, the plasma region volume expands, producing a more uniform particle distribution. On the other hand, increasing power results in higher the electron density and complete ionization of gas molecules, further contributing to a more uniform plasma distribution.

Figure 6(b) illustrates the relationship between the uniformity degree and the source power. The uniformity degree increases with the increase in the source power. Moreover, the plasma radial uniformity exhibits a slower growth rate with increasing gas pressure. This phenomenon occurs because electrons near the coil are heated as source power increases, leading to a rise in the uniformity degree

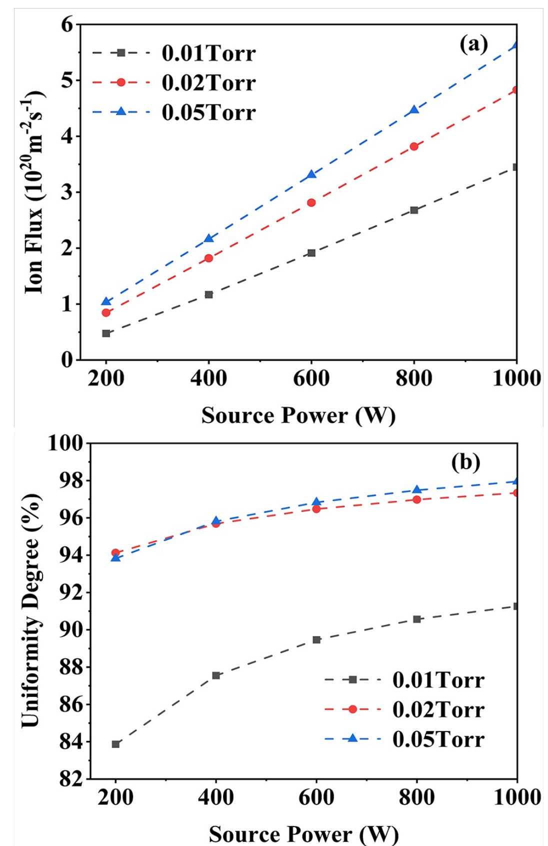

Figure 6. Source power dependence of (a) the ion flux and (b) the uniformity degree at different gas pressures.

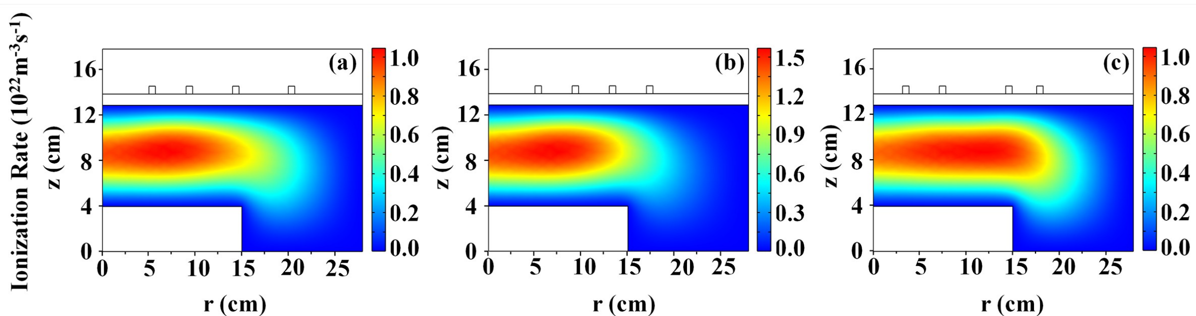

Figure 5. Distributions of ionization rate for different coil radial spacings. (a) Step coil, (b) isometric coil, and (c) optimized coil.

from 84% to 98%. This increase suggests a more uniform electron density distribution. Consequently, increasing the source power can improve the plasma uniformity.

Figure 7(a) illustrates the dependence of gas pressure on ion flux above the substrate, ranging from 0.01 Torr to 0.05 Torr, under constant source powers of 200 W, 500 W and 800 W. It is observed that higher source powers result in higher ion fluxes. Moreover, the ion flux grows slowly with the variation of gas pressure at lower source power, such as 200 W. However, at higher power levels, such as 800 W, there is a tendency for the ion flux to increase with higher gas pressure. It occurs because the likelihood of electron collisions with gas molecules increases as gas pressure increases, resulting in more energy being utilized in the ionization reaction. In addition, the electron density changes from an edge-high distribution to a center-high distribution, which shows that the uniformity of the plasma improves.

For instance, as shown in figure 7(a), the ion flux increases from 2.68×10^{20} m^{-2} s^{-1} to 4.47×10^{20} m^{-2} s^{-1} under the fixed power of 800 W. Similarly, as depicted in figure 7(b), the uniformity degree rises from 91% to 97% as the gas pressure increases. It implies that the radial uniformity of the plasma becomes progressively better with increasing gas pressure. Therefore, higher gas pressure should be selected to ensure better plasma uniformity. Moreover, figure 7(b) shows that as the gas pressure further increases, the effect of local heating of electrons becomes more significant, the spatial distribution of plasma density is restricted, and the uniformity growth slows down and possibly even shows a downward trend. These findings suggest that both source power and gas pressure are crucial factors in enhancing plasma radial uniformity, with the effect of source power being particularly notable.

3.2. Effect of chamber aspect ratio on plasma uniformity

The chamber aspect ratio is also a critical parameter of ICP. In prior research, we investigated the effects of various chamber structures on plasma density distribution in the Penning ion gauge ion source [32]. Building upon this research, we chose the ICP reactor with an isometric coil configuration for further investigation. The subsequent analysis concentrates on the influence of chamber structural parameters, particularly the chamber aspect ratio, on electron density distribution and plasma radial uniformity. The simulations were conducted under initial conditions of 500 W and 0.02 Torr to maintain consistency.

To further explore the modulation of plasma uniformity by the chamber aspect ratio, the chamber aspect ratio k is defined here as the ratio of the chamber radius (r) to the chamber height (h), i.e., the aspect ratio $k = r/h$. The distributions of electron densities for different values of k are plotted in figures 8 and 9. There is a striking disparity in the plasma uniformity. In the case of $k = 2.8$, although the electron density peak increases from 1.48×10^{17} m^{-3} to 1.8×10^{17} m^{-3}, the distribution of electron densities has a similar trend to the initial conditions. The radial uniformity of the

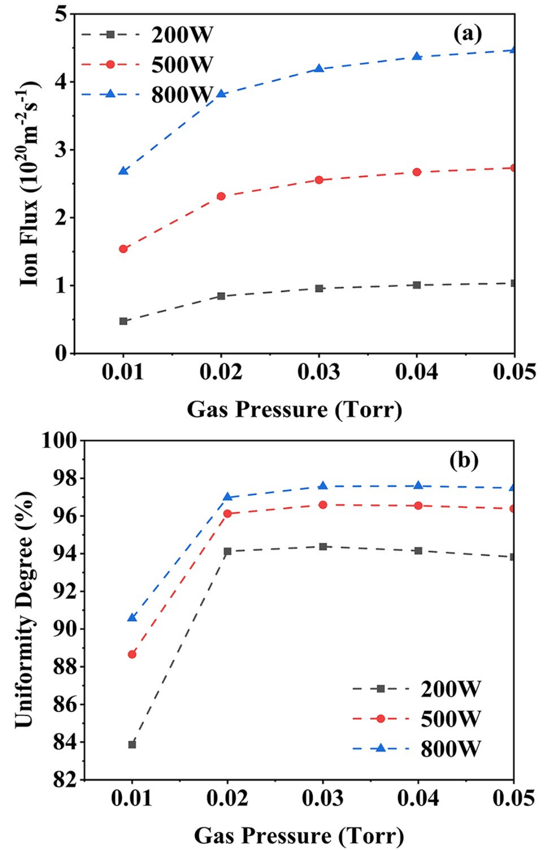

Figure 7. Gas pressure dependence of (a) the ion flux and (b) the uniformity degree at different source powers.

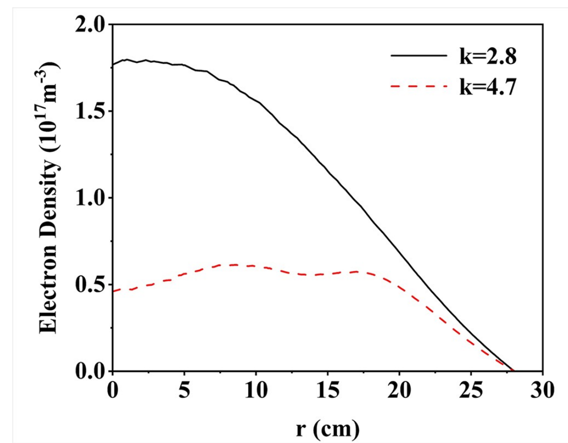

Figure 8. Radial distributions of electron density for different values of k.

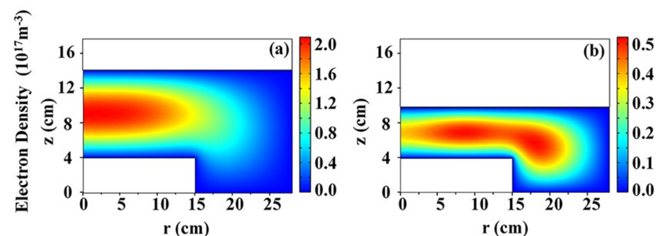

Figure 9. Distributions of electron density for different values of k. (a) $k = 2.8$, (b) $k = 4.7$.

plasma remains relatively constant, exhibiting no substantial changes, as seen in figures 9(a) and 4(b).

However, for k = 4.7, figure 9(b) demonstrates that the electron densities at positions r = 8 cm and r = 17 cm show two distinct peaks in its radial distribution. At the same time, the electron density value decreases by almost one order of magnitude compared to k = 2.8. The uniformity degree is 84%, meaning there is no noticeable change in the plasma uniformity. These observations suggest that the electrons below the coil are heated more locally, and the interaction of charged particles with the walls increases in relatively small chamber volumes, increasing in surface losses, which causes the total electron density to decrease. Due to the increase in ionization rate, the electron temperature increases to maintain the plasma. In addition, the plasma region is compressed due to reduced chamber volume, increasing the collision frequency between electrons and gas molecules and changing the plasma distribution. The electron density changes from center-high to saddle-shaped and gradually approaches the edge distribution as the k increases. In other words, the plasma uniformity gradually becomes worse.

It is observed that the ionization rate also changes significantly for different values of k. As seen in figure 10(a), the distribution of ionization rates has a similar trend with the initial conditions (see figure 5(b)) at k = 2.8. However, in the case of k = 4.7 (see figure 10(b)), the peak of the ionization rate moves outwards off-axis and reaches a maximum at r = 8 cm. It occurs because most power deposition takes place beneath the dielectric window where the internal coil is situated, leading to electron heating by an induced electric field. With reduced chamber volume and uneven electric field distribution, electrons may accumulate enough energy in localized areas to initiate ionization process, resulting in an elevated ionization rate. Moreover, as the value of k increases, the ionization rate shifts from a center-high distribution to an edge-high distribution. On the other hand, the plasma uniformity degree calculations indicate that plasma uniformity initially improves and then sharply declines with increasing k.

In this subsection, to further explore the mechanisms that influence plasma uniformity, the ICP reactor with chamber aspect ratio k = 4.7 configuration is presented for further analysis. In order to research the effect of process parameters, such as source power and gas pressure, on the ion flux and the plasma uniformity, it is observed that the ion flux increases as source power increases under fixed gas pressure. Moreover, a more notable growth rate is observed at higher gas pressures, as shown in figure 11(a). For example, there is a significant increase in ion flux from 0.87 × 10^{20} m^{-2} s^{-1} to 5.11 × 10^{20} m^{-2} s^{-1} when source power is increased from 200 W to 1000 W at 0.05 Torr. The increase in source power translates to more energy reaching the plasma region, thereby providing electrons with increased energy for ionization process. The increase in source power causes the electron collision frequency to increase, which helps to increase the energy of the ions, increasing in the ion flux. On the other hand, increasing source power also raises the electron density, and ensures complete ionization of gas molecules, thereby promoting a more uniform plasma distribution.

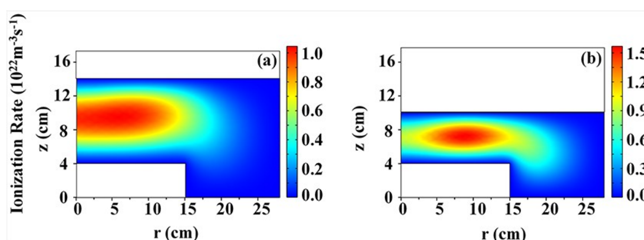

Figure 10. Distributions of ionization rate for different k. (a) k = 2.8, (b) k = 4.7.

Additionally, plasma uniformity increases with increasing source power at lower gas pressures, such as 0.01 Torr, but the increase is less significant at higher gas pressures, such as 0.05 Torr. The variation of plasma uniformity degree with source power is shown in figure 11(b). The plasma uniformity is at its lowest at 200 W and 0.01 Torr, with a uniformity degree of 10%, and at its highest at 1000 W and 0.02 Torr, reaching 88%. It demonstrates that higher gas pressure does not necessarily yield a better uniformity degree when increasing source power. Selecting the appropriate gas pressure while increasing source power is crucial to achieve better plasma uniformity.

The gas pressure dependence of the ion flux at different source powers is obtained when k = 4.7, as seen in figure 12(a), resembling figure 7(a). Ion flux demonstrates a posi-

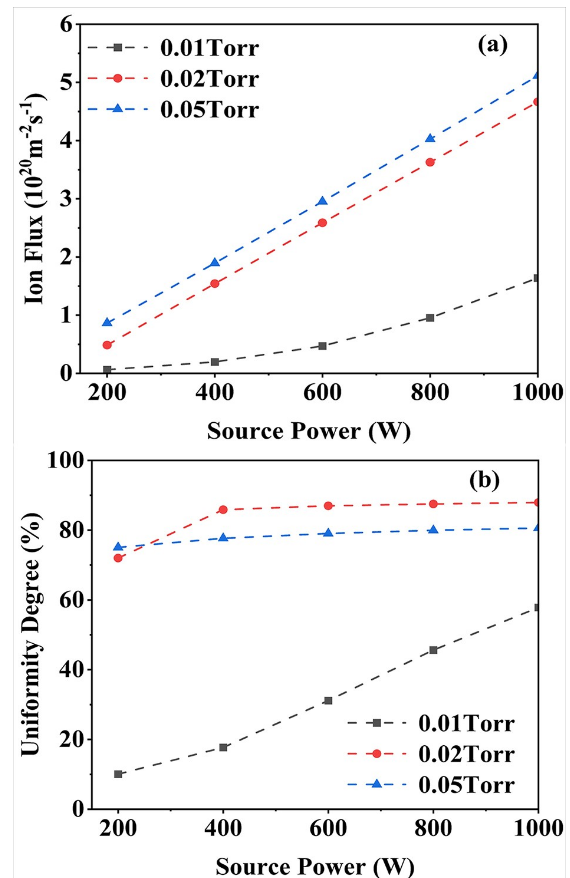

Figure 11. Source power dependence of (a) the ion flux and (b) the uniformity degree at different gas pressures.

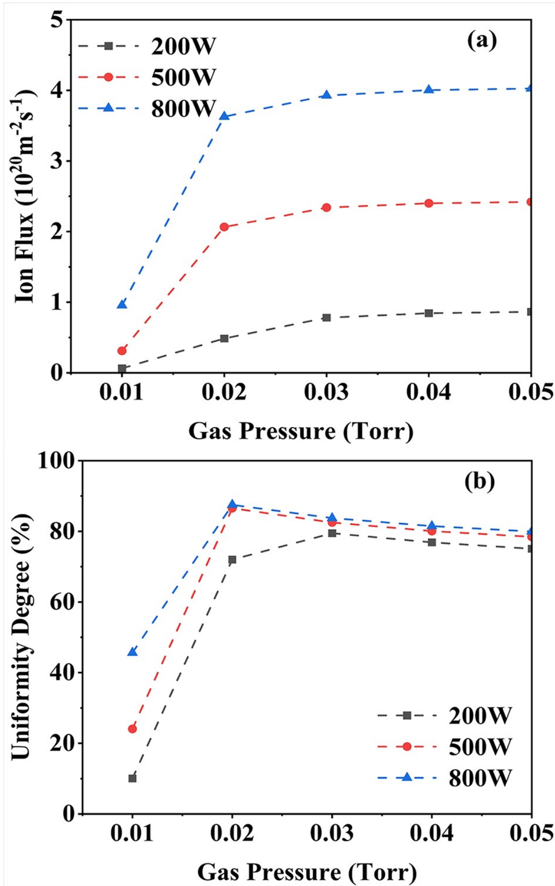

Figure 12. Gas pressure dependence of (a) the ion flux and (b) the uniformity degree at different source powers.

tive correlation with gas pressure at fixed source power, with the most notable increase observed at gas pressures ranging from 0.01 Torr to 0.02 Torr. For instance, the ion flux increases rapidly from 0.96×10^{20} m^{-2} s^{-1} to 3.63×10^{20} m^{-2} s^{-1} at 800 W. The frequency of collisions of ions with gas molecules increases significantly as the gas pressure increases. These collisions offer ions the chance to acquire energy, amplifying both their velocity and energy of ion motion, consequently boosting the ion flux. On the other hand, the ionization rate also increases significantly under higher gas pressure conditions, leading to the generation of more ions. At the same time, the peaks of the ion fluxes all occurred at 0.05 Torr. The phenomenon suggests that higher source power leads to increased ion flux.

In addition, the plasma density changes significantly with increasing gas pressure. It can be seen that the plasma uniformity is also well improved as the gas pressure is raised from 0.01 Torr to 0.02 Torr. For instance, the uniformity degree increases from 10% to 72% at the fixed source power of 200 W, as shown in figure 12(b). However, the uniformity degree decreases as the gas pressure increases to 0.05 Torr. The uniformity degree decreases from 87% at 0.02 Torr to 78% at 0.05 Torr at a fixed source power of 500 W. The best uniformity degree is achieved with a value of 88% at 0.02 Torr and 800 W. This highlights that increasing source power appropriately can lead to a better plasma uniformity degree when the gas pressure is fixed.

4. Conclusions

This study investigates the impact of various coil configurations and chamber aspect ratios on plasma parameters and radial uniformity through the development of a two-dimensional fluid model. Concurrently, it explores the influence of process parameters on plasma radial uniformity within the coil and chamber structures, respectively.

First, the plasma radial uniformity is modulated in ICP generators with different coil configurations by adjusting the radial spacing. The results show that in the case of optimized coil configurations, the plasma uniformity degree is increased from 56% to 96% compared to the initial conditions, producing better plasma radial uniformity. As a result, the electron density distribution is influenced by the different coil configurations. Therefore, altering the coil radial spacing can improve the plasma uniformity. In addition, the uniformity degree grows from 94% to 98% as the source power is increased from 200 W to 1000 W at 0.05 Torr. Similarly, the uniformity degree grows from 91% to 97% when the gas pressure is increased from 0.01 Torr to 0.05 Torr at 800 W. This suggests that alterations in process parameters enhance plasma uniformity.

The plasma radial uniformity is modulated in ICP generators with different chamber structures by adjusting the chamber aspect ratio. The results show that in the case of k = 4.7, the plasma uniformity degree is increased from 83% to 84% compared to the initial conditions, and plasma uniformity is not a significant improvement. In this case, the electron density changes from a center-high to a saddle-shaped distribution. It is shown that a larger chamber aspect ratio means the reactor has a smaller chamber volume, and the plasma region is compressed, affecting the plasma distribution. In addition, in the context of ion flux dependence on source power, the uniformity degree increases from 72% to 88% when transitioning from 200 W to 1000 W for the source power at 0.02 Torr. Similarly, regarding the influence of the gas pressure on ion flux, the uniformity degree rises from 46% to 88% with the gas pressure increment from 0.01 Torr to 0.02 Torr at 800 W. Where the impact of source power is more pronounced.

Based on the simulation findings of this research, it can be concluded that adjusting the coil and chamber construction can enhance the uniformity degree. Thereby improving plasma radial uniformity. This research is a valuable reference for designing ICP sources in plasma etching processes.

Acknowledgments

This work was supported by the Scientific Research Foundation of Xijing University, China (No. XJ19T03), the Opening Project of Science and Technology on Reliability Physics and Application Technology of Electronic Component Laboratory (No. ZHD201701), and the Natural Science Basic Research Plan in Shaanxi Province of China (No. 2024J C-YBMS-342).

References

[1] Hopwood J 1992 *Plasma Sources Sci. Technol.* **1** 109
[2] Lee H C 2018 *Appl. Phys. Rev.* **5** 011108
[3] Mackie N M *et al* 1997 *Chem. Mater.* **9** 349
[4] Park J H *et al* 2006 *Appl. Phys. Lett.* **89** 121108
[5] Charles C 2009 *J. Phys. D: Appl. Phys.* **42** 163001
[6] Mazouffre S 2016 *Plasma Sources Sci. Technol.* **25** 033002
[7] Hagelaar G J M, Fubiani G and Boeuf J P 2011 *Plasma Sources Sci. Technol.* **20** 015001
[8] Boeuf J P *et al* 2011 *Plasma Sources Sci. Technol.* **20** 015002
[9] Santoso J *et al* 2015 *Phys. Plasmas* **22** 093513
[10] Sun X Y *et al* 2021 *Plasma Sci. Technol.* **23** 095404
[11] Son E J, Cho S H and Lee H J 2020 *J. Electr. Eng. Technol.* **15** 2259
[12] Xiao D Z *et al* 2020 *Surf. Coat. Technol.* **400** 126252
[13] Lu C *et al* 2023 *Phys. Plasmas* **30** 063506
[14] Collison W Z, Ni T Q and Barnes M S 1998 *J. Vac. Sci. Technol. A* **16** 100
[15] Kim K N *et al* 2006 *Appl. Phys. Lett.* **89** 251501
[16] Gweon G H *et al* 2010 *Vacuum* **84** 823
[17] Mishra A *et al* 2012 *Plasma Sources Sci. Technol.* **21** 035018
[18] Yang K C *et al* 2019 *Vacuum* **168** 108802
[19] Levko D, Shukla C and Raja L L 2021 *J. Vac. Sci. Technol. B* **39** 062204
[20] Stittsworth J A and Wendt A E 1996 *Plasma Sources Sci. Technol.* **5** 429
[21] Hao Z Y *et al* 2020 *Phys. Plasmas* **27** 043502
[22] Mirza M M *et al* 2012 *J. Vac. Sci. Technol. B* **30** 06FF02
[23] Li J S *et al* 2008 *J. Appl. Phys.* **103** 043505
[24] Wächter A and Biegler L T 2006 *Math. Program.* **106** 25
[25] Bukowski J D, Graves D B and Vitello P 1996 *J. Appl. Phys.* **80** 2614
[26] Lee I, Graves D B and Lieberman M A 2008 *Plasma Sources Sci. Technol.* **17** 015018
[27] Wang Y J *et al* 2021 *Plasma Sci. Technol.* **23** 115602
[28] Si X J *et al* 2011 *Phys. Plasmas* **18** 033504
[29] Sobolewski M A and Kim J H 2007 *J. Appl. Phys.* **102** 113302
[30] Zhou J C *et al* 2022 *Vacuum* **195** 110678
[31] Zhang Y R, Hu Y T and Wang Y N 2020 *Plasma Sources Sci. Technol.* **29** 084003
[32] Li J *et al* 2020 *J. Phys.: Conf. Ser.* **1601** 022044